Low-cycle fatigue of 10 % Cr steel with high boron content at room temperature

Ivan S. Brazhnikov*[1], engineer
of the Joint Research Center of Belgorod State National Research University "Technology and Materials"
Alexandra E. Fedoseeva[2], PhD (Engineering),
senior researcher of the Laboratory of Mechanical Properties of Nanostructured Materials and Superalloys
Belgorod State National Research University, Belgorod (Russia)

*E-mail: 1216318@bsu.edu.ru

[1]ORCID: https://orcid.org/0009-0008-8069-7376
[2]ORCID: https://orcid.org/0000-0003-4031-463X

Abstract: High-chromium martensitic steels are a promising material for the production of elements of boilers and steam pipelines, as well as blades and rotors of steam turbines for new coal-burning thermal generating units. The use of such materials will give an opportunity for the transition to ultra-supercritical steam parameters (temperature of 600–620 °C and pressure of 25–30 MPa), which will allow increasing the efficiency of generating units to 45 %. Modifications of the chemical composition of high-chromium steels have led to significant improvements of high-temperature properties such as 100,000 h creep strength and 1 % creep limit, while resistance to softening due to low-cycle fatigue remains understudied in this field. This work covers the study of low-cycle fatigue at room temperature with different amplitudes of deformation of martensitic high-chromium 10%Cr–3%Co–2%W–0.5%Mo–0.2%Cu–0.2%Re–0.003%N–0.01%B steel. The steel was pre-subjected to normalizing at 1050 °C followed by tempering at 770 °C. After heat treatment, the steel structure was a tempered martensitic lath structure stabilised by the particles of secondary phases of $M_{23}C_6$ carbides, NbX carbonitrides, and M_6C carbides. The average width of martensite laths was 380 nm, and the dislocation density was 1.4×10^{14} m^{-2}. At low-cycle fatigue, with an increase in the strain amplitude from 0.2 to 1 %, the number of cycles before failure significantly decreases, and the value of plastic deformation in the middle of the number of loading cycles significantly increases. Maximum softening (18 %) is observed at a strain amplitude of 1 % in the middle of the number of loading cycles. In general, the steel structure after low-cycle fatigue tests does not undergo significant changes: the width of the laths increases by 18 % at a strain amplitude of more than 0.3 %, while the dislocation density remains at a rather high level (about 10^{14} m^{-2}) at all strain amplitudes.

Keywords: martensitic heat-resistant steel; low-cycle fatigue; strain amplitude; fatigue softening; fatigue failure.

Acknowledgements: The work was financially supported by the Russian Science Foundation (Agreement No. 19-73-10089-П). Link to information about the project: https://rscf.ru/project/22-73-41001/.

The authors express their gratitude to the Joint Research Center of Belgorod State National Research University "Technology and Materials" for the equipment provided for carrying out structural studies.

The paper was written on the reports of the participants of the XI International School of Physical Materials Science (SPM-2023), Togliatti, September 11–15, 2023.

For citation: Brazhnikov I.S., Fedoseeva A.E. Low-cycle fatigue of 10 % Cr steel with high boron content at room temperature. *Frontier Materials & Technologies*, 2024, no. 2, pp. 33–42. DOI: 10.18323/2782-4039-2024-2-68-3.

INTRODUCTION

9–12 % Cr steels are considered as promising materials for the production of elements of new thermal generating units, operating at super-supercritical steam parameters (temperature of 600–620 °C, pressure of 25–30 MPa) [1]. The transition to new super-supercritical steam parameters will increase the efficiency of thermal generating units to 45 % [2; 3].

The structure of 9–12 % Cr steels is a tempered lath troostite, the boundaries of which are fixed by particles of $M_{23}C_6$ carbides (where M is Cr, Fe, and Mo), and the high density of dislocations inside the martensitic laths is held by fine *MX* carbonitrides (where *M* is V and/or Nb, *X* is C and/or N) [4; 5]. It has been found that adding a small amount of boron to chromium-molybdenum and chromium-tungsten steels can significantly increase creep resistance [6; 7]. Segregation of boron at the boundaries of the prior austenite grains (PAG) strengthens and prevents local softening of these boundaries under creep conditions [6; 7]. Moreover, adding boron reduces the rate of coarsening of $M_{23}C_6$ carbides precipitated at the boundaries of martensite laths, blocks, packets, and PAG [8]. On the other hand, in steels with a high nitrogen content, boron tends to form large particles of boron nitride BN, which act as sources of cracks and discontinuities during creep [1].

Along with the BN formation in steels with a high nitrogen content, small metastable particles of *MX* carbonitrides are transformed into large particles of the thermodynamically stable Z-phase (Cr(V,Nb)N) during creep, which negatively affects the properties [9]. Reducing the nitrogen content to very small values (less than 0.003 wt. %) solves two problems at once: 1) prevention of the formation of large BN and Z-phase particles, and 2) the possibility of increasing the boron content to 0.01 wt. %. In this case, a significant

increase in original austenite grains up to 50–60 μm occurs [10]. The addition of cobalt, tungsten, molybdenum, and rhenium to steel slows down diffusion-controlled processes during creep, such as the Laves phase formation, particle coarsening and lath coarsening, which also has a positive effect on creep resistance [11; 12]. This approach to alloying can make it possible to increase the long-term creep strength from 72 (for P92 steel [13]) to 100 MPa [14].

Good creep resistance is demonstrated by the new promising 10 % Cr martensitic steel, which was chosen to be studied in this work. Thus, the long-term strength limit of the steel under study was 93 MPa at 650 °C on a basis of 100,000 h; moreover, there is no discontinuity in the long-term strength curve [12]. However, during operation of steam turbine blades, low-cycle fatigue cracks can form [1].

Currently, there are quite a lot of works covering the study of low-cycle fatigue of high-chromium steels [15–17]. High-chromium steels typically exhibit three distinct stages during low-cycle fatigue tests: a rapid softening stage, a stable stage, and a stage of final failure due to the initiation and propagation of cracks [15; 18–20]. In [15], it was found that when increasing test temperature, the proportion of plastic deformation increases, especially at large strain amplitudes. The structure of the material with increasing temperature of low-cycle fatigue test also undergoes significant changes, such as the formation of subgrains and the evolution of the dislocation structure – from cellular at room temperature to wall-like at elevated temperatures [19]. An increase in test temperature causes an increase in the distance between martensitic laths [16]. When tested for low-cycle fatigue at room temperature, fatigue softening depends on the size of the laths and is associated with dynamic recrystallisation [20].

Since the steel under study is supposed to be used as a material for the production of steam turbine blades, a detailed study of the creep characteristics is not enough. Low-cycle fatigue behaviour should be included in the study. The results concerning the behaviour of 10%Cr–3%Co–2W–0.5Mo–0.2Cu–0.2Re–0.003N–0.01B steel when tested for low-cycle fatigue will be useful for determining permissible cyclic loads, during operation of parts of thermal power plants made from the steels under study.

The purpose of this work is to identify the influence of the strain amplitude magnitude during low-cycle fatigue on the structural changes of 10 % Cr martensitic steel at room temperature.

METHODS

Table 1 presents the chemical composition of the new 10 % Cr martensitic steel. The steel was cast at the LLC SMSM plant, Moscow, in a vacuum induction furnace.

After peeling, the ingots were homogenised at a temperature of 1150 °C for 16 h, followed by forging at the same temperature into blanks in the form of square bars with a square side of 50 mm, followed by cooling in air. Heat treatment of steel included normalizing at a temperature of 1050 °C for 1 h, cooling in air, followed by tempering at a temperature of 770 °C for 3 h, cooling in air.

Low-cycle fatigue tests were carried out on cylindrical samples in accordance with GOST 25.502-79, with a working part diameter of 5 mm and a reduced gauge length of up to 18 mm. The decrease in the gauge length of the sample is caused by the tendency of martensitic steel samples to longitudinal bending during compression at high strain amplitudes. Tension-compression tests were carried out with an asymmetry coefficient (R) of −1 at room temperature, with strain amplitudes of 0.2, 0.3, 0.6, and 1 % and a frequency of 0.5 Hz using an Instron 8801 testing machine (Great Britain). One sample was used for each amplitude. The study of the microstructure in the initial state, and after low-cycle fatigue tests was carried out on a JEM JEOL-2100 transmission electron microscope (Japan), equipped with an energy-dispersive spectrometer, at an accelerating voltage of 200 kV. The foils for microstructure studies were cut from the area closest to the fracture zone. The density of free dislocations inside the laths was determined from the number of dislocation exit points on the foil surface. The size of martensite laths was determined by the random secant method in six randomly selected areas of the structure. The equilibrium volume fraction of secondary phase particles was determined using Thermo-Calc software (TCFE7 database) (Sweden).

RESULTS

Structure after heat treatment

As a result of heat treatment, a rather homogeneous tempered martensitic lath structure is formed in 10 % Cr steel (Fig. 1 a). The average transverse size of martensite laths was (380±30) nm. Inside the laths, both free dislocations (Fig. 1 c) and networks of dislocations (Fig. 1 b) are observed. The dislocation density inside the laths is quite high and amounts to $(1.4\pm0.5)\times10^{14}\,\mathrm{m}^{-2}$. Analysis of the replicas (Fig. 1 d) showed that during the heat treatment, particles of $M_{23}C_6$ carbides enriched in chromium, particles of *MX* carbonitrides enriched in niobium, and a very small amount of particles of M_6C carbides enriched in tungsten are released. $M_{23}C_6$ carbides are the dominant phase and precipitate along the boundaries of original austenite grains, packets, blocks and martensite laths. Their average size is (70±5) nm, volume fraction – 2.35 %.

Table 1. Chemical composition of 10%Cr–3%Co–2W–0.5Mo–0.2Cu–0.2Re–0.003N–0.01B steel, wt. %
Таблица 1. Химический состав стали 10%Cr–3%Co–2W–0,5Mo–0,2Cu–0,2Re–0,003N–0,01B, вес. %

Fe	C	Cr	Co	W	Mo	Cu	V	Nb	Re	B	N
Base	0.13	9.4	3.1	2.1	0.6	0.29	0.16	0.05	0.17	0.015	0.002

NbX carbonitrides with an average size of 30 nm are uniformly distributed throughout the material volume (Fig. 1 d). M_6C carbides with an average size of 40 nm were found along the boundaries of martensite laths (Fig. 1 d). The volume fractions of the last two phases are insignificant and do not exceed 0.1 %.

Properties during low-cycle fatigue at room temperature

Fig. 2 presents the results of low-cycle fatigue tests at room temperature. At a minimum strain amplitude of 0.2 %, the number of cycles before failure was 213,822 (Fig. 2 a). For the steel under study, as the strain amplitude increases, the number of cycles before failure decreases significantly. Thus, even a slight increase in the strain amplitude from 0.2 to 0.3 % reduces the number of cycles by 1 order of magnitude (Fig. 2 a). A further increase in the strain amplitude from 0.3 to 0.6 % reduces the number of cycles by another 8 times (Fig. 2 a). At the largest strain amplitude of 1 %, the number of cycles before failure decreased to 488 cycles (Fig. 2 a).

When comparing the number of cycles before failure during low-cycle fatigue of the steel under study to other 9–10 % Cr steels [21–23] at strain amplitudes of 0.3 and 0.6 %, it was found that at a strain amplitude of 0.3 %, the steel under study demonstrates 14,411 cycles to failure (Fig. 2 b). This correlates well with the values of cycles before failure for other steels [21–23]. On the other hand, at a strain amplitude of 0.6 %, the steel under study shows 1,815 cycles before failure, which exceeds the number of cycles before failure for the steels presented in [21–23] more than 2 times.

The hysteresis loops during low-cycle fatigue tests have an asymmetry, and with increasing strain amplitude, the hysteresis loop asymmetry increases. At a strain amplitude of 0.2 %, fatigue failure occurs mainly during elastic deformation, which, combined with the number of cycles before failure exceeding 200,000, allows classifying this test as a high-cycle fatigue test (Fig. 3). The stress amplitude in this case is 396.3 MPa. With an increase in the strain amplitude from 0.2 to 1 %, the contribution of the strain plastic component increases, and destruction occurs in the elastoplastic area (Table 2). With an increase in the strain amplitude from 0.2 to 1 %, the increase in the stress amplitude was 30 %, while the amplitude of the strain plastic component increased by 95 times.

During low-cycle fatigue tests at room temperature, cyclic hardening of the steel under study occurs, which is expressed in an increase in the stress amplitude with an increase in the number of cycles in relation to the first cycle stress (Fig. 4 a). This is typical for all strain amplitudes. For example, at a strain amplitude of 0.2 %, the steel under study was hardened up to the 60th cycle, and the same level of stress amplitude was maintained until failure. At a strain amplitude of 1 %, the steel strengthened up to 6 cycles, after which a decrease in the stress amplitude was observed relative to the first cycle (Fig. 4 a). A decrease in the stress amplitude relative to the first cycle stress indicates material softening. On the other hand, such a decrease in stress amplitude relative to the first cycle stress may be caused by a decrease in force due to necking (reduction in cross-sectional area).

One can see that at a strain amplitude of 0.2 %, the degree of softening is negative, which indicates that up to 50 % of the total number of cycles before failure, the stress amplitude is higher than the first cycle stress amplitude (Fig. 4 b). However, even with a slight increase in the strain amplitude to 0.3 %, the value of the material stress amplitude becomes lower than the first cycle stress by already 5 % of the total number of cycles before failure. In this case, the degree of softening increases twice at 50 % of the total number of cycles before failure.

It should be noted that with a strain amplitude of 0.6 %, the degree of fatigue softening even at 50 % of the total number of cycles before failure does not exceed 10 % and is comparable to an amplitude of 0.3 %. At an amplitude of 1 %, the maximum softening of the steel under study is observed, which is 18 % at 40 and 50 % of the total number of cycles before failure.

Fractography of fractures

The relative reduction of samples after low-cycle fatigue increases significantly from 5 to 20 % for an amplitude from 0.2 to 1 %, which is caused by an increase in the strain plastic component. On the fracture surface, two zones can be clearly distinguished: the fatigue failure area and the rupture area (final destruction) (Fig. 5). Fatigue grooves can be discerned in the fatigue failure area. The rupture area has a viscous character expressed by small pits. An evaluation of the proportion of the fatigue failure area in relation to the entire fracture surface, revealed that this value does not depend on the strain amplitude and ranges from 45 to 60 %.

Structure after low-cycle fatigue

After low-cycle fatigue tests at all strain amplitudes, the tempered martensitic lath structure formed during heat treatment is preserved (Fig. 6). After low-cycle fatigue tests with a strain amplitude of 0.2 % (the number of cycles is more than 200,000), the average width of the laths is (370±30) nm, which coincides with the value before the test (Table 3). In this case, the density of free dislocations inside martensite laths also does not change compared to the initial state and amounts to $(1.4\pm0.5)\times10^{14}$ m^{-2} (Table 3).

With an increase in the strain amplitude up to 1 %, an insignificant increase in the width of martensite laths up to (460±30) nm is observed (Table 2), which is caused by the appearance of a strain plastic component (Table 1). Let us remark, that the dislocation density changes at the error level with increasing strain amplitude. The absence of significant changes in the dispersions of particles of secondary phases after low-cycle fatigue tests is also worth noting.

DISCUSSION

The number of cycles before failure at a strain amplitude of 0.2 % has passed the conventional threshold of 5×10^4 cycles, which indicates a transition from the low-cycle fatigue area to the high-cycle fatigue area. However, when the strain amplitude increases to 1 %, the number of
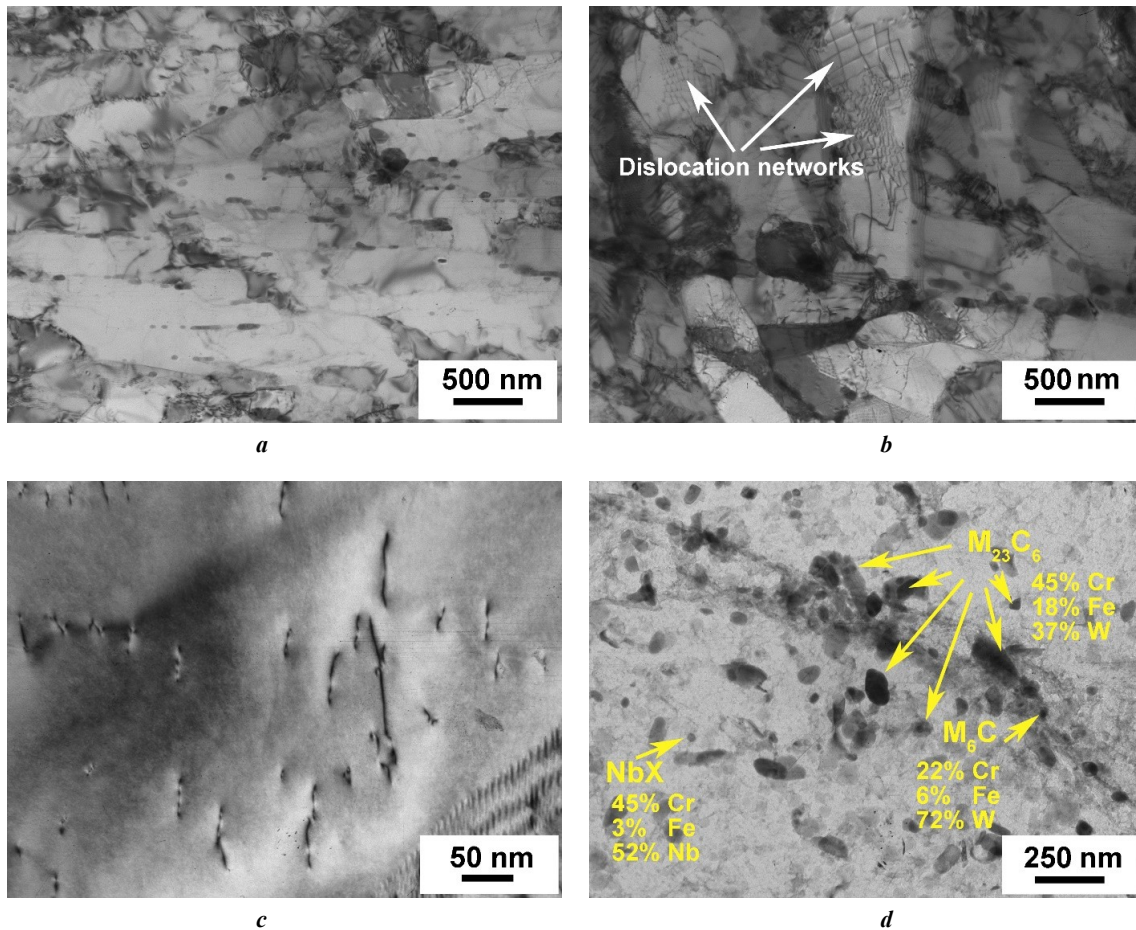
Fig. 1. *Images of the microstructure of the 10 % Cr steel under study after heat treatment,*
*obtained by TEM method of thin foils (**a–c**) and carbon replicas (**d**)*
Рис. 1. *Изображения микроструктуры исследуемой 10 % Cr стали после термической обработки,*
*полученные методом ПЭМ тонких фольг (**a–c**) и углеродных реплик (**d**)*
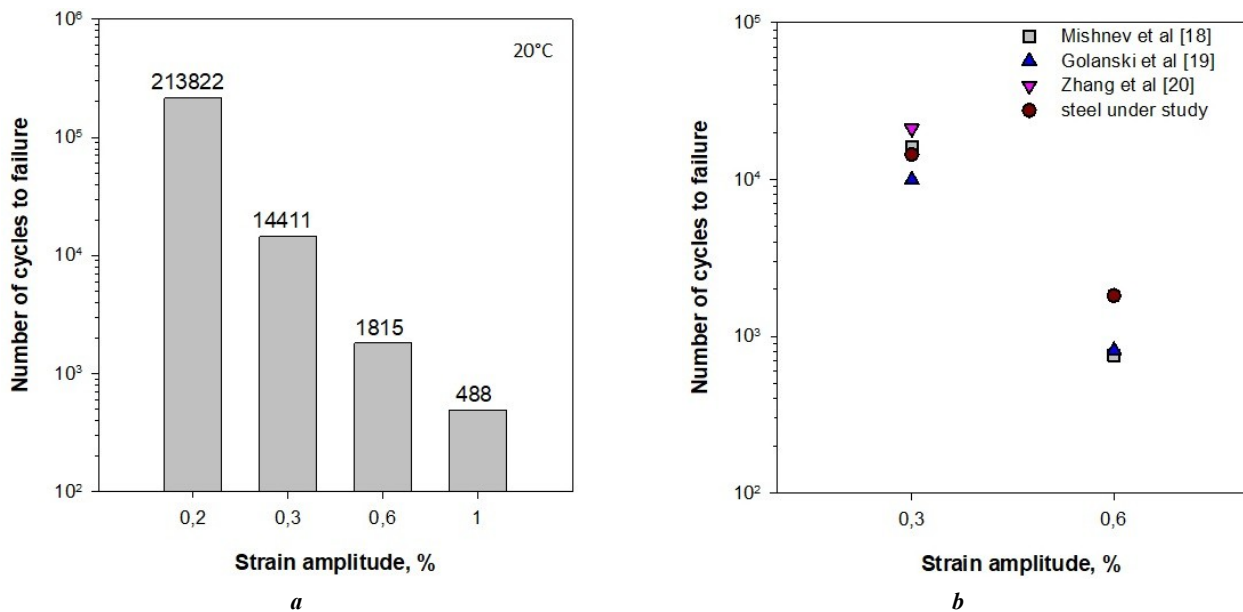
Fig. 2. *Dependence of the number of cycles to failure on the strain amplitude for the steel under study (**a**)*
and a comparison of the number of cycles to failure during low-cycle fatigue of the steel under study
*with other 9–10 % Cr steels [21–23] at strain amplitudes of 0.3 and 0.6 % (**b**)*
Рис. 2. *Зависимость количества циклов до разрушения от амплитуды деформации для исследуемой стали (**a**),*
а также сравнение количества циклов до разрушения при малоцикловой усталости исследуемой стали
*с другими 9–10 % Cr сталями [21–23] при амплитудах деформации 0,3 и 0,6 % (**b**)*
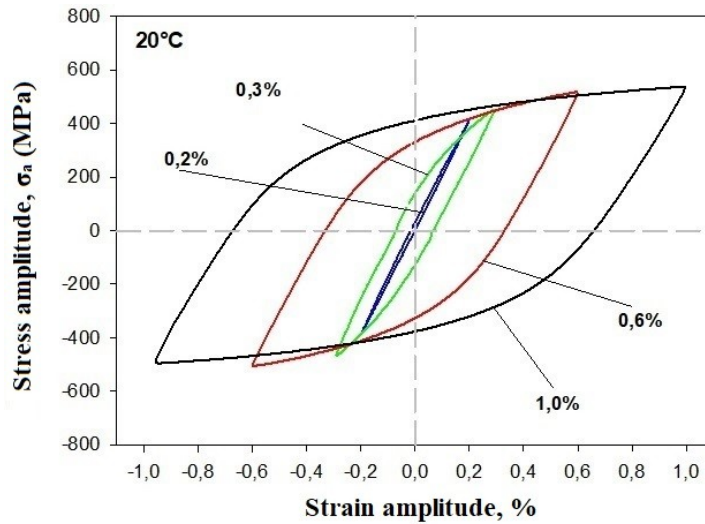
Fig. 3. *"Stress amplitude – strain amplitude" hysteresis loops*
in the middle of the number of loading cycles at a test temperature of 20 °C for 10 % Cr steel
Рис. 3. *Петли гистерезиса «Амплитуда напряжения – амплитуда деформации»*
в середине количества циклов нагружения при температуре испытания 20 °C для 10 % Cr стали

Table 2. *Data of low-cycle fatigue in the middle of the number of loading cycles*
Таблица 2. *Данные малоцикловой усталости в середине количества циклов нагружения*

Characteristics of low cycle fatigue	Strain amplitude ε_{ac}, %			
	0.2	**0.3**	**0.6**	**1**
Stress amplitude, $\sigma_a \dfrac{N}{2}$, MPa	396.3	459.8	511.1	515.7
Amplitude of strain plastic component ε_{ap}, %	0.007	0.073	0.33	0.666

a

b
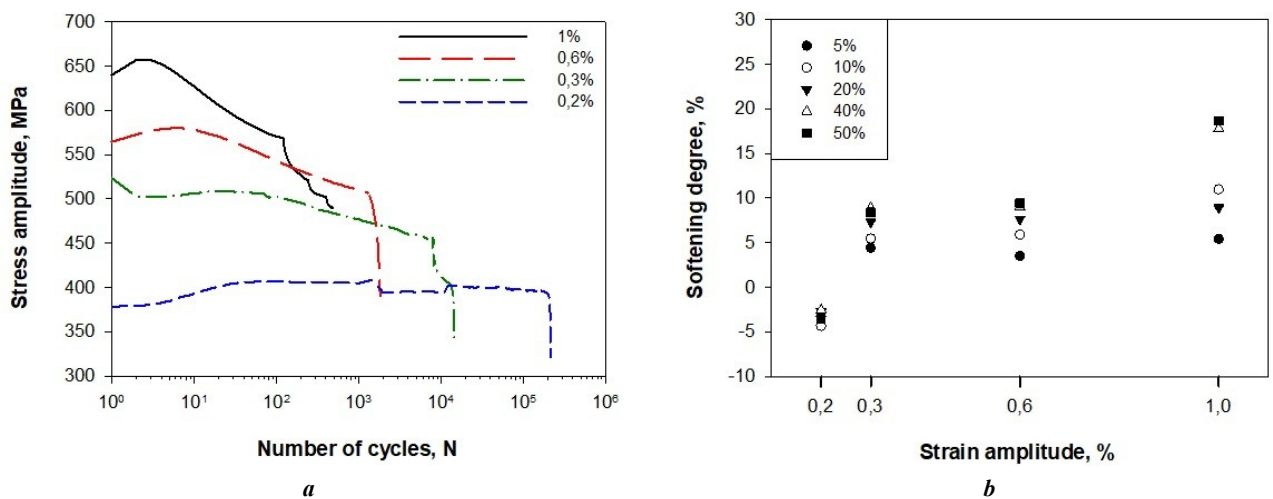
Fig. 4. *Dependence of the stress amplitude on the number of cycles at a strain amplitude of 0.2, 0.3, 0.6, and 1 % (**a**)*
together with the degree of fatigue softening in relation to the first cycle stress at different fractions
*of the maximum number of cycles before failure (**b**)*
Рис. 4. *Зависимость амплитуды напряжения от количества циклов при амплитуде деформации 0,2; 0,3; 0,6 и 1 % (**a**)*
совместно со степенью циклического разупрочнения по отношению к напряжению первого цикла при различных долях
*от максимального количества циклов до разрушения (**b**)*
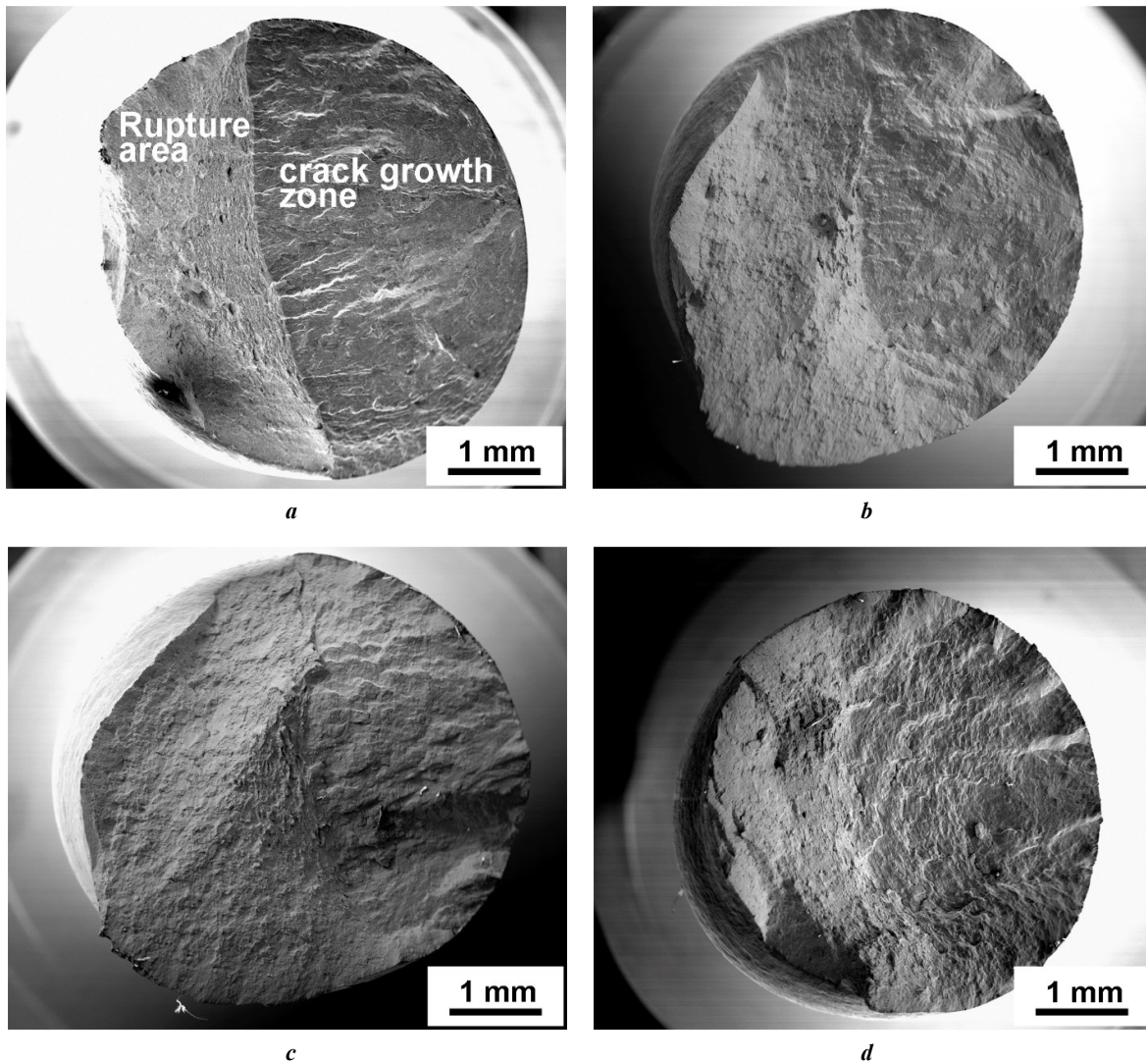
Fig. 5. *Fractography of fractures of destroyed samples after low-cycle fatigue tests*
*at strain amplitudes of 0.2 % (**a**), 0.3 % (**b**), 0.6 % (**c**), and 1 % (**d**)*
Рис. 5. *Фрактография изломов разрушенных образцов после испытаний на малоцикловую усталость*
*при амплитудах деформации 0,2 % (**a**), 0,3 % (**b**), 0,6 % (**c**) и 1 % (**d**)*

cycles before failure does not exceed 2×10^4 cycles, which indicates that for this steel, tests with a given strain amplitude above 0.3 % remain in the low-cycle fatigue area. Loop asymmetry in Fig. 3 is associated with the Bauschinger effect: the wider the loop, the greater the Bauschinger strain [21]. For the steel under study, one can note that with an increase in the strain amplitude in the middle of the number of loading cycles, the hysteresis loop width increases. It should be noted that at a strain amplitude of 0.2 %, the hysteresis loop is almost symmetrical, and accordingly, the Bauschinger strain in this case is extremely small. Thus, the loop width at a strain amplitude of 0.2 % clearly demonstrates, predominantly, elastic strain during the test.

The absence of transformations of lath boundaries into subgrain boundaries through the interaction of lath boundaries, and free dislocations is caused by the low test temperature. At room temperature, interaction even between free dislocations proceeds slowly [22]. Long-range fields of elastic stresses from dislocations and low-

angle lath boundaries prevent the capture of dislocations by boundaries [21], which leads to the absence of visible changes in the structure after low-cycle fatigue tests at a strain amplitude of 0.2 %. Moreover, such a structure demonstrates cyclic hardening (Fig. 4). It is worth noting that cyclic hardening in the first cycles at room temperature is also observed in [21]. On the contrary, +24 % broadening of martensite laths after low-cycle fatigue testing at higher strain amplitudes, due to the appearance of a strain plastic component, can lead to fatigue softening (Fig. 4). Thus, substructural hardening from martensite laths can be assessed using the Langford–Cohen equation [24]:

$$\sigma_{\text{laths}} = \frac{k_h}{2l},$$

where k_h is the hardening coefficient (0.0862 MPa×m [24]); l is the width of martensite laths.
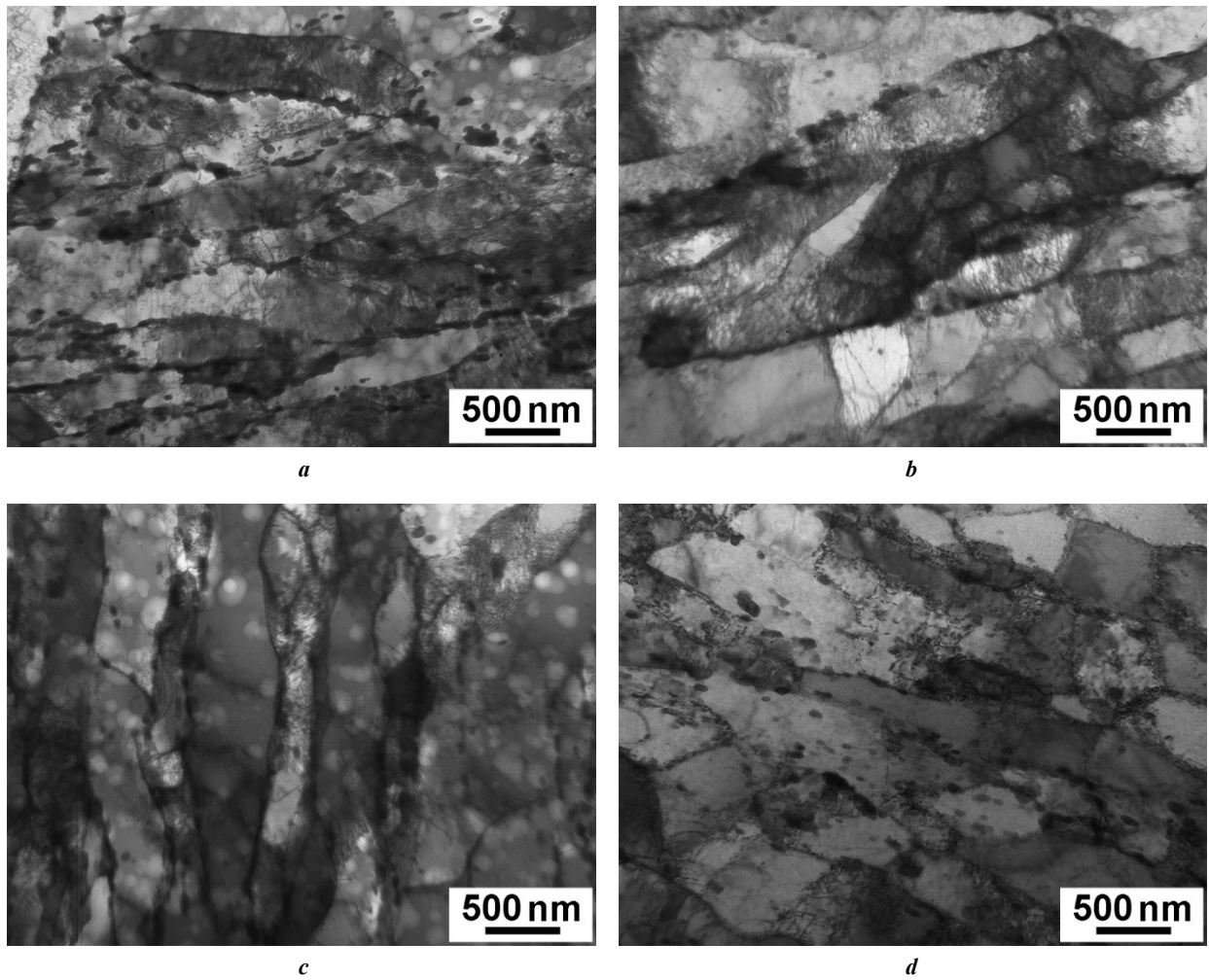
Fig. 6. Microstructure of the steel under study after low-cycle fatigue testing
*at strain amplitudes of 0.2 % (**a**), 0.3 % (**b**), 0.6 % (**c**), and 1 % (**d**)*
***Рис. 6.** Микроструктура исследуемой стали после испытания на малоцикловую усталость*
*при амплитудах деформации 0,2 % (**a**), 0,3 % (**b**), 0,6 % (**c**) и 1 % (**d**)*

Table 3. *Microstructural parameters of 10%Cr–3%Co–2W–0.5Mo–0.2Cu–0.2Re–0.003N–0.01B steel*
after low-cycle fatigue tests
Таблица 3. *Микроструктурные параметры стали 10%Cr–3%Co–2%W–0,5%Mo–0,2%Cu–0,2%Re–0,003%N–0,01%В*
после испытания на малоцикловую усталость

Strain amplitude, %	0.2	0.3	0.6	1
Dislocation density, $\times 10^{14}$ m^{-2}	1.4±0.5	2.4±0.5	1.1±0.5	1.9±0.5
Lath width, nm	370±30	450±30	460±30	460±30

The magnitude of hardening in the initial state was 113 MPa (with a lath width of 380 nm (Table 3)), while lath broadening to 450–460 nm after low-cycle fatigue at 0.3–1 % of the strain amplitude (Table 3), leads to a decrease in substructural hardening up to 94–96 MPa. On the other hand, an increase in the relative reduction (reduction of cross-sectional area) causes a decrease in force rather than stress, which can be expressed as an apparent decrease in strain stress after necking. Thus, with an amplitude of 1 %,

the relative reduction reaches 20 %, and softening occurs by approximately the same amount.

To identify the nature of the softening, Table 4 summarizes the values of softening caused by the broadening of the laths, the relative reduction values, and the values of the decrease in stress amplitude for a certain cycle in comparison with the first loading cycle. A comparison of the data from Table 4 showed that the softening of the material during low-cycle fatigue at high strain

Table 4. *The values of softening due to the widening of the laths, relative reduction and the decrease in the stress amplitude for a certain cycle compared to the first loading cycle for various strain amplitudes, %*
Таблица 4. *Величины разупрочнения из-за уширения реек, относительного сужения и значения снижения амплитуды напряжения для определенного цикла в сравнении с первым циклом нагружения для различных амплитуд деформаций, %*

Strain amplitude	0.2	0.3	0.6	1
Softening due to the widening of martensite laths	–	15	17	17
Relative reduction	5	12	8	20
Decrease in the stress amplitude relative to the first cycle stress at 50 % of the total number of cycles before failure	–	8	9	19

amplitudes is caused by the beginning of an increase in relative reduction (reduction of cross-sectional area), and not by a structural factor.

CONCLUSIONS

It has been found that an increase in the strain amplitude from 0.2 to 1 % reduces the number of cycles before failure by 3 orders of magnitude. The maximum softening of 18 % is observed at a strain amplitude of 1 % in the middle of the number of loading cycles. At the same time, the steel under study, after low-cycle fatigue tests, retains the tempered martensitic lath structure formed during heat treatment without significant changes. The material softening is caused by the beginning of an increase in the relative reduction of the samples.

REFERENCES

1. Kaybyshev R.O., Skorobogatykh V.N., Shchenkova I.A. New martensitic steels for fossil power plant: creep resistance. *The Physics of Metals and Metallography*, 2010, vol. 109, no. 2, pp. 186–200. EDN: MXPLYJ.
2. Abe F., Kern T.-U., Viswanathan R. *Creep-resistant steels*. Cambridge, Woodhead Publishing, 2008. 800 p.
3. Kern T.U., Staubli M., Scarlin B. The European efforts in material development for 650 °C USC power plants-COST522. *ISIJ international*, 2002, vol. 42, no. 12, pp. 1515–1519. DOI: 10.2355/isijinternational.42.1515.
4. Bladesha H.K.D.H., Design of ferritic creep-resistant steels. *ISIJ international*, 2001, vol. 41, no. 6, pp. 626–640. DOI: 10.2355/isijinternational.41.626.
5. Kostka A., Tak K.-G., Hellmig R.J., Estrin Y., Eggeler G. On the contribution of carbides and micrograin boundaries to the creep strength of tempered martensite ferritic steels. *Acta Materialia*, 2007, vol. 55, no. 2, pp. 539–550. DOI: 10.1016/j.actamat.2006.08.046.
6. Abe F. Effect of boron on microstructure and creep strength of advanced ferritic power plant steels. *Procedia Engineering*, 2011, vol. 10, pp. 94–99. DOI: 10.1016/j.proeng.2011.04.018.
7. Takahashi N., Fujita T. The Effect of Boron on the Long Period Creep Rupture Strength of the Modified 12% Chromium Heat Resisting Steel. *Transactions of the Iron and Steel Institute of Japan*, 1976, vol. 16, no. 11, pp. 606–613. DOI: 10.2355/isijinternational1966.16.606.
8. Kaibyshev R., Mishnev R., Fedoseeva A., Dudova N. The role of microstructure in creep strength of 9-12% Cr steels. *Materials Science Forum*, 2017, vol. 879, pp. 36–41. DOI: 10.4028/www.scientific.net/MSF.879.36.
9. Danielsen H.K. Review of Z phase precipitation in 9–12 wt-% Cr steels. *Materials Science and Technology*, 2016, vol. 32, no. 2, pp. 126–137. DOI: 10.1179/1743284715Y.0000000066.
10. Nikitin I.S., Fedoseeva A.E. Effect of the Normalizing Temperature on the Short-Time Creep of Martensitic 10Cr–3Co–3W–0.2Re Steel with a Low Nitrogen Content. *Russian Metallurgy (Metally)*, 2022, vol. 2022, pp. 753–763. DOI: 10.1134/S0036029522070102.
11. Knezevic V., Balun J., Sauthoff G., Inden G., Schneider A. Design of martensitic/ferritic heat-resistant steels for application at 923 K with supporting thermodynamic modeling. *Materials Science and Engineering: A*, 2008, vol. 477, no. 1-2, pp. 334–343. DOI: 10.1016/j.msea.2007.05.047.
12. Fedoseeva A.E. Creep Resistance and Structure of 10% Cr–3% Co–2% W–0.29% Cu–0.17% Re Steel with Low Nitrogen and High Boron Contents for Unit Components of Coal Power Plants. *Physical Mesomechanics*, 2024, vol. 27, pp. 88–101. DOI: 10.1134/S1029959924010090.
13. Haarmann K., Vaillant J.C., Vandenberghe B., Bendick W., Arbab A. *The T92/P92 Book*. Boulogne, Vallourec and Mannesmann tubes Publ., 1998. 62 p.
14. Dudova N., Mishnev R., Kaibyshev R. Creep behavior of a 10%Cr heat-resistant martensitic steel with low nitrogen and high boron contents at 650 °C. *Materials Science and Engineering: A*, 2019, vol. 766, article number 138353. DOI: 10.1016/j.msea.2019.138353.
15. Wang Quanyi, Wang Qingyuan, Gong Xiufang, Wang Tianjian, Zhang Wei, Li Lang, Liu Yongjie, He Chao, Wang Chong, Zhang Hong. A comparative study of low cycle fatigue behavior and microstructure of Cr-based steel at room and high temperatures. *Materials & Design*, 2020, vol. 195, article number 109000. DOI: 10.1016/j.matdes.2020.109000.
16. Zhang Zhe, Li Xiaofei, Yu Yaohua, Li Bingbing, Zhang Bo, Ma Yushan, Chen Xu. Effects of temperature and strain amplitude on low-cycle fatigue behavior of 12Cr13 martensitic stainless steel. *Journal of Materials Research and Technology*, 2024, vol. 29, pp. 1414–1427. DOI: 10.1016/j.jmrt.2024.01.162.
17. Mao Jianfeng, Zhu Jian, Li Xiangyang, Wang Dasheng, Zhong Fengping, Chen Jichang. Effect of strain ampli-

tude and temperature on creep-fatigue behaviors of 9–12% Cr steel. *Journal of Mechanical Science and Technology*, 2022, vol. 36, no. 5, pp. 2265–2276. DOI: 10.1007/s12206-022-0409-y.

18. Chen Furen, Zhang Wei, Zhang Kaihao, Yang Qiaofa, Wang Xiaoxiao, Zhou Changyu. Low cycle fatigue and creep-fatigue interaction behavior of 2.25CrMoV steel at high temperature. *Journal of Materials Research and Technology*, 2024, vol. 28, pp. 3155–3165. DOI: 10.1016/j.jmrt.2023.12.233.

19. Shi Shouwen, Cui Jianpeng, Li Haiyan, Chen Gang, Lin Qiang, Chen Xu. Cyclic stress response and microcrack initiation mechanism of modified 9Cr1Mo steel under low cycle fatigue at room temperature and 350 °C. *Fatigue and Fracture of Engineering Materials and Structures*, 2023, vol. 46, no. 7, pp. 2525–2538. DOI: 10.1111/ffe.14015.

20. Zhang Xiaodong, Wang Tianjian, Gong Xiufang, Li Qingsong, Liu Yongjie, Wang Quanyi, Zhang Hong, Wang Qingyuan. Low cycle fatigue properties, damage mechanism, life prediction and microstructure of MarBN steel: Influence of temperature. *International Journal of Fatigue*, 2021, vol. 144, article number 106070. DOI: 10.1016/j.ijfatigue.2020.106070.

21. Mishnev R., Dudova N., Kaibyshev R. Low cycle fatigue behavior of a 10Cr–2W–Mo–3Co–NbV steel. *International Journal of Fatigue*, 2016, vol. 83-2, pp. 344–355. DOI: 10.1016/j.ijfatigue.2015.11.008.

22. Golański G., Mroziński S. Low cycle fatigue and cyclic softening behaviour of martensitic cast steel. *Engineering Failure Analysis*, 2013, vol. 35, pp. 692–702. DOI: 10.1016/j.engfailanal.2013.06.019.

23. Zhang Zhen, Hu Zheng-fei, Fan Li-kun, Wang Bin. Low cycle fatigue behavior and cyclic softening of P92 ferritic-martensitic steel. *Journal of Iron and Steel Research International*, 2015, vol. 22, pp. 534–542. DOI: 10.1016/S1006-706X(15)30037-6.

24. Langford G., Cohen M. Strain hardening of iron by severe plastic deformation. *American Society for Metals Transactions*, 1969, vol. 62, pp. 623–638.

СПИСОК ЛИТЕРАТУРЫ

1. Кайбышев Р.О., Скоробогатых В.Н., Щенкова И.А. Новые стали мартенситного класса для тепловой энергетики. Жаропрочные свойства // Физика металлов и металловедение. 2010. Т. 109. № 2. С. 200–215. EDN: LOIWVD.

2. Abe F., Kern T.-U., Viswanathan R. Creep-resistant steels. Cambridge: Woodhead Publishing, 2008. 800 p.

3. Kern T.U., Staubli M., Scarlin B. The European efforts in material development for 650 °C USC power plants – COST522 // ISIJ international. 2002. Vol. 42. № 12. P. 1515–1519. DOI: 10.2355/isijinternational.42.1515.

4. Bladesha H.K.D.H., Design of ferritic creep-resistant steels // ISIJ international. 2001. Vol. 41. № 6. P. 626–640. DOI: 10.2355/isijinternational.41.626.

5. Kostka A., Tak K.-G., Hellmig R.J., Estrin Y., Eggeler G. On the contribution of carbides and micrograin boundaries to the creep strength of tempered martensite ferritic steels // Acta Materialia. 2007. Vol. 55. № 2. P. 539–550. DOI: 10.1016/j.actamat.2006.08.046.

6. Abe F. Effect of boron on microstructure and creep strength of advanced ferritic power plant steels // Procedia Engineering. 2011. Vol. 10. P. 94–99. DOI: 10.1016/j.proeng.2011.04.018.

7. Takahashi N., Fujita T. The Effect of Boron on the Long Period Creep Rupture Strength of the Modified 12% Chromium Heat Resisting Steel // Transactions of the Iron and Steel Institute of Japan. 1976. Vol. 16. № 11. P. 606–613. DOI: 10.2355/isijinternational1966.16.606.

8. Kaibyshev R., Mishnev R., Fedoseeva A., Dudova N. The role of microstructure in creep strength of 9-12% Cr steels // Materials Science Forum. 2017. Vol. 879. P. 36–41. DOI: 10.4028/www.scientific.net/MSF.879.36.

9. Danielsen H.K. Review of Z phase precipitation in 9–12 wt-% Cr steels // Materials Science and Technology. 2016. Vol. 32. № 2. P. 126–137. DOI: 10.1179/1743284715Y.0000000066.

10. Nikitin I.S., Fedoseeva A.E. Effect of the Normalizing Temperature on the Short-Time Creep of Martensitic 10Cr–3Co–3W–0.2Re Steel with a Low Nitrogen Content // Russian Metallurgy (Metally). 2022. Vol. 2022. P. 753–763. DOI: 10.1134/S0036029522070102.

11. Knezevic V., Balun J., Sauthoff G., Inden G., Schneider A. Design of martensitic/ferritic heat-resistant steels for application at 923 K with supporting thermodynamic modeling // Materials Science and Engineering: A. 2008. Vol. 477. № 1-2. P. 334–343. DOI: 10.1016/j.msea.2007.05.047.

12. Fedoseeva A.E. Creep Resistance and Structure of 10% Cr–3% Co–2% W–0.29% Cu–0.17% Re Steel with Low Nitrogen and High Boron Contents for Unit Components of Coal Power Plants // Physical Mesomechanics. 2024. Vol. 27. P. 88–101. DOI: 10.1134/S1029959924010090.

13. Haarmann K., Vaillant J.C., Vandenberghe B., Bendick W., Arbab A. The T92/P92 Book. Boulogne: Vallourec and Mannesmann tubes, 1998. 62 p.

14. Dudova N., Mishnev R., Kaibyshev R. Creep behavior of a 10%Cr heat-resistant martensitic steel with low nitrogen and high boron contents at 650 °C // Materials Science and Engineering: A. 2019. Vol. 766. Article number 138353. DOI: 10.1016/j.msea.2019.138353.

15. Wang Quanyi, Wang Qingyuan, Gong Xiufang, Wang Tianjian, Zhang Wei, Li Lang, Liu Yongjie, He Chao, Wang Chong, Zhang Hong. A comparative study of low cycle fatigue behavior and microstructure of Cr-based steel at room and high temperatures // Materials & Design. 2020. Vol. 195. Article number 109000. DOI: 10.1016/j.matdes.2020.109000.

16. Zhang Zhe, Li Xiaofei, Yu Yaohua, Li Bingbing, Zhang Bo, Ma Yushan, Chen Xu. Effects of temperature and strain amplitude on low-cycle fatigue behavior of 12Cr13 martensitic stainless steel // Journal of Materials Research and Technology. 2024. Vol. 29. P. 1414–1427. DOI: 10.1016/j.jmrt.2024.01.162.

17. Mao Jianfeng, Zhu Jian, Li Xiangyang, Wang Dasheng, Zhong Fengping, Chen Jichang. Effect of strain amplitude and temperature on creep-fatigue behaviors of 9–12% Cr steel // Journal of Mechanical Science and Technology. 2022. Vol. 36. № 5. P. 2265–2276. DOI: 10.1007/s12206-022-0409-y.

18. Chen Furen, Zhang Wei, Zhang Kaihao, Yang Qiaofa, Wang Xiaoxiao, Zhou Changyu. Low cycle fatigue and creep-fatigue interaction behavior of 2.25CrMoV steel at high temperature // Journal of Materials

Research and Technology. 2024. Vol. 28. P. 3155–3165. DOI: 10.1016/j.jmrt.2023.12.233.

19. Shi Shouwen, Cui Jianpeng, Li Haiyan, Chen Gang, Lin Qiang, Chen Xu. Cyclic stress response and microcrack initiation mechanism of modified 9Cr1Mo steel under low cycle fatigue at room temperature and 350 °C // Fatigue and Fracture of Engineering Materials and Structures. 2023. Vol. 46. № 7. P. 2525–2538. DOI: 10.1111/ffe.14015.

20. Zhang Xiaodong, Wang Tianjian, Gong Xiufang, Li Qingsong, Liu Yongjie, Wang Quanyi, Zhang Hong, Wang Qingyuan. Low cycle fatigue properties, damage mechanism, life prediction and microstructure of MarBN steel: Influence of temperature // International Journal of Fatigue. 2021. Vol. 144. Article number 106070. DOI: 10.1016/j.ijfatigue.2020.106070.

21. Mishnev R., Dudova N., Kaibyshev R. Low cycle fatigue behavior of a 10Cr–2W–Mo–3Co–NbV steel // International Journal of Fatigue. 2016. Vol. 83-2. P. 344–355. DOI: 10.1016/j.ijfatigue.2015.11.008.

22. Golański G., Mroziński S. Low cycle fatigue and cyclic softening behaviour of martensitic cast steel // Engineering Failure Analysis. 2013. Vol. 35. P. 692–702. DOI: 10.1016/j.engfailanal.2013.06.019.

23. Zhang Zhen, Hu Zheng-fei, Fan Li-kun, Wang Bin. Low cycle fatigue behavior and cyclic softening of P92 ferritic-martensitic steel // Journal of Iron and Steel Research International. 2015. Vol. 22. P. 534–542. DOI: 10.1016/S1006-706X(15)30037-6.

24. Langford G., Cohen M. Strain hardening of iron by severe plastic deformation // American Society for Metals Transactions. 1969. Vol. 62. P. 623–638.

Малоцикловая усталость 10 % Cr стали с высоким содержанием бора при комнатной температуре

*Бражников Иван Сергеевич**[1], инженер
Центра коллективного пользования «Технологии и Материалы НИУ "БелГУ"»
Федосеева Александра Эдуардовна[2], кандидат технических наук,
старший научный сотрудник лаборатории механических свойств наноструктурных и жаропрочных материалов
Белгородский государственный национальный исследовательский университет, Белгород (Россия)

*E-mail:** 1216318@bsu.edu.ru

[1]ORCID: https://orcid.org/0009-0008-8069-7376
[2]ORCID: https://orcid.org/0000-0003-4031-463X

Аннотация: Высокохромистые стали мартенситного класса являются перспективным материалом для изготовления элементов котлов и паропроводов, а также лопаток и роторов паровых турбин новых энергоблоков тепловых электростанций, работающих на угле. Использование таких материалов даст возможность осуществить переход на суперсверхкритические параметры пара (температура 600–620 °С и давление 25–30 МПа), что позволит увеличить КПД энергоблоков до 45 %. Модификации химического состава высокохромистых сталей привели к существенному повышению жаропрочных характеристик, таких как предел длительной прочности – до 100 000 ч и предел ползучести – до 1 % на базе 100 000 ч, в то время как сопротивление разупрочнению в результате малоцикловой усталости остается недостаточно изученным в данной области. Настоящая работа посвящена исследованию малоцикловой усталости при комнатной температуре с различными амплитудами деформации высокохромистой стали мартенситного класса 10%Cr–3%Co–2%W–0,5%Mo–0,2%Cu–0,2%Re–0,003%N–0,01%B. Предварительно сталь была подвергнута нормализации с 1050 °С с последующим отпуском при 770 °С. После термической обработки структура стали представляла собой реечный троостит отпуска, стабилизированный частицами вторичных фаз карбидов $M_{23}C_6$, карбонитридов NbX и карбидов M_6C. Средняя ширина мартенситных реек составляла 380 нм, а плотность дислокаций – $1,4\times10^{14}$ м$^{-2}$. При малоцикловой усталости с увеличением амплитуды деформации с 0,2 до 1 % значительно снижается количество циклов до разрушения, а значение пластической деформации в середине количества циклов нагружения существенно увеличивается. Максимальное разупрочнение (18 %) наблюдается при амплитуде деформации 1 % в середине количества циклов нагружения. В целом структура стали после испытаний на малоцикловую усталость не претерпевает существенных изменений: ширина реек увеличивается на 18 % при амплитуде деформации более 0,3 %, при этом плотность дислокаций сохраняется на достаточно высоком уровне (около 10^{14} м$^{-2}$) при всех амплитудах деформации.

Ключевые слова: жаропрочная сталь мартенситного класса; малоцикловая усталость; амплитуда деформации; циклическое разупрочнение; усталостное разрушение.